

Influence of the donor doping density in CdS and Zn(O,S) buffer layers on the external quantum efficiency of Cu(In,Ga)Se₂ thin film solar cell

Alain Kassine EHEMBA[#], Moustapha DIENG[#], Demba DIALLO[#], Gerome SAMBOU[#]

[#]Laboratory of Semiconductors and Solar Energy, Physics Department, Faculty of Science and Technology University Cheikh Anta Diop – Dakar - SENEGAL

Abstract — In this paper, we study the influence of the donor doping density of the buffer layer on external quantum efficiency EQE. We simulate a Cu(In,Ga)Se₂ thin film solar cell using the AMPS. We use two types of buffer layer: the Zn(O,S) and the CdS. These layers are doped N with various doping densities going from 10¹⁵cm⁻³ to 10²⁰cm⁻³. The variation of external quantum efficiency shows us that for the doping densities going from 10¹⁵cm⁻³ to 10¹⁷cm⁻³, the Zn(O,S) buffer layer gives more powerful properties than those of the CdS buffer layer. For the doping densities higher than 10¹⁷cm⁻³, the Zn(O,S) and CdS layers give properties which make them competing. They present maximum absorption areas extended on broad wavelength ranges. We note an EQE which can reach 100% for the cells with the Zn(O,S) buffer layer and 98.6% for the cells with the CdS buffer layer. Then the Zn(O, S) buffer layer gives better quantum efficiency according to its doping density even if the CdS buffer layer is more known.

Keywords — buffer layer, donor density, CdS, Zn(O,S), Cu(In,Ga)Se₂, external quantum efficiency EQE.

I. INTRODUCTION

In the bibliography, we note that the use of the CdS like buffer layer in solar cells elaboration was carried out before that of Zn(O,S) buffer layer. Many work was carried out in the direction to elucidate the importance of the properties which offer the Zn(O,S) used in the place of CdS [1]-[3]. The principal interest of the Zn(O,S) use resides on the fact that it presents an optical gap larger than the CdS one. We note also the fact that its conduction band offset CBO can be optimized. This optimization is possible while exploiting the Oxygen/Sulfide ratio [4].

Several methods of elaboration are used to deposit the Zn(O,S) layer such as Chemical Bath Deposition (CBD) [2], Atomic Layer Deposition (ALD) [5] and Magnetron Deposition [6]. Several methods were also used to deposit the CdS buffer layer. The more frequent elaboration method of Zn(O,S) is the CBD [7].

The doping density of these two buffer layers has an influence on the electric parameters of the solar cell, in particular the short circuit current density [8] and the quantum efficiency [9]. We are interested by the

influence of donor doping density of buffer layer on external quantum efficiency. The external quantum efficiency EQE is the ratio of the number of carriers collected on the number of incidental photons. The characterization of the cell by its quantum efficiency makes it possible to do without the studies of transmittance and reflectance. It is a significant parameter for the characterization which was already used in our former work [10].

II. EXPERIMENTAL PROCESS

This paper is based on a simulation carried out using the AMPS. It is a software developed by Fonash et al. [11]-[12]. It is conceived for the thin film solar cell simulation. The layers of these structures can be monocrystal, polycrystal, amorphous or combinations. The types of studied cells are indicated by figure 1.

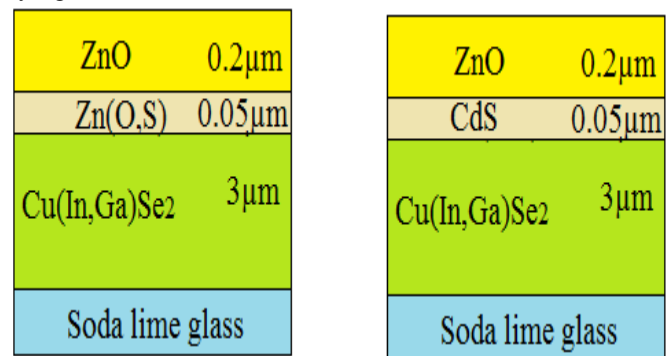


Fig. 1: The two types of studied cells

The properties of the CdS and Zn(O,S) buffer layers are given by table 1.

Tab. 1: Some properties of the buffer layers

Buffer layer	Gap (E _g)	Electronic Affinity	ΔE=E _c -E _v
CdS	2.40eV	4.20eV	1.58×10 ¹⁹ eV
Zn(O, S)	3.3eV	4.45V	1.58×19 ¹⁹ eV

The two buffer layers have the same thickness. The most influential parameter on quantum efficiency is the material gap. The absorption of the photons is mainly based on their wavelength. The gap of each buffer layer absorbs on a well definite wavelength range. We can evaluate the wavelength applying the formula:

$$E = \frac{hC}{\lambda} \quad (1) \quad \Rightarrow \quad \lambda = \frac{hC}{E} \quad (2)$$

The CdS gap corresponds then to a wavelength of 517nm and that of Zn(O,S) corresponds to a wavelength of 370nm. From the simulated cells we can obtain the characteristics of external quantum efficiency. We study the variation of this last according to the donor doping density of the buffer layers. The doping density is a very influential parameter on the electric parameters of the cells. It is used as batch-setup. We vary it from 10^{15}cm^{-3} to 10^{20}cm^{-3} and we use incidental wavelengths going from 200nm to 1400nm.

The study is undertaken under a spectrum of illumination AM1.5 which corresponds to an incidental illumination of 1000W.m^{-2} and a transmission of 100%.

The Cu(In, Ga)Se₂ constitutes the active zone of the CdS/Cu(In, Ga)Se₂ and Zn(O, S)/Cu(In, Ga)Se₂ heterojunctions. It is the zone where the majority of the surplus minority carriers is generated.

III. RESULTS AND DISCUSSIONS

A. External quantum efficiency of the cells with buffer layers doped $N_d=10^{15} \text{cm}^{-3}$.

The figure 2 gives quantum efficiencies of the solar cells with CdS and Zn(O,S) buffer layers. These two materials are doped N with a doping density of 10^{15}cm^{-3} .

The quantum efficiency of the cell with the CdS buffer layer gives a characteristic less broad than that obtained with the cell with Zn(O,S) buffer layer. The low wavelengths going from 200nm to 363nm correspond to incidental photons of significant energy. They give weak quantum efficiency because the number of carriers is still weak. Always with the CdS

buffer layer, from 363nm the quantum efficiency becomes significant. It reaches maximum of 98% for an incidental wavelength of 570nm. This wavelength corresponds to energy of 2.17eV. The number of collected carriers is maximum and the short circuit current density is maximum. Until 600nm the injection level of incidental wavelengths gives a significant quantum efficiency. From this value it drops quickly to reduce to zero with $\lambda=689\text{nm}$. This phenomenon can be explained by the fact that it is formed on the energy band diagram of the cell a spike at the conduction band offset. This spike constitutes a barrier for the photogenerated carriers wish raise the fall of quantum yield.

Concerning the quantum efficiency of the cell with a Zn(O, S) buffer layer we have a broader characteristic. From 200nm to 363nm quantum efficiency remains low because these wavelengths correspond to the incidental photons of significant energy. These photons take part more in the rise of the cell than to the creation of carriers open to be collected. For the wavelengths higher than 363nm, external quantum efficiency increases fastly to reach 100% for a wavelength of 422nm. This corresponds to the maximum absorption area which extends until the gap of Cu(In, Ga)Se₂. For wavelengths lower than this gap, incidental energy is insufficient for the creation of carriers. Then we observe the fall of the quantum efficiency which is reduced to zero for $\lambda=1192\text{nm}$ which corresponds to an incidental energy of 1.04eV.

B. External quantum efficiency of the cells with buffer layers doped $N_d=10^{16} \text{cm}^{-3}$.

The Figure 3 gives the quantum efficiency of the cells with CdS and Zn(O,S) buffer layers doped N with doping density equal to 10^{16}cm^{-3} . The doping density remains medium.

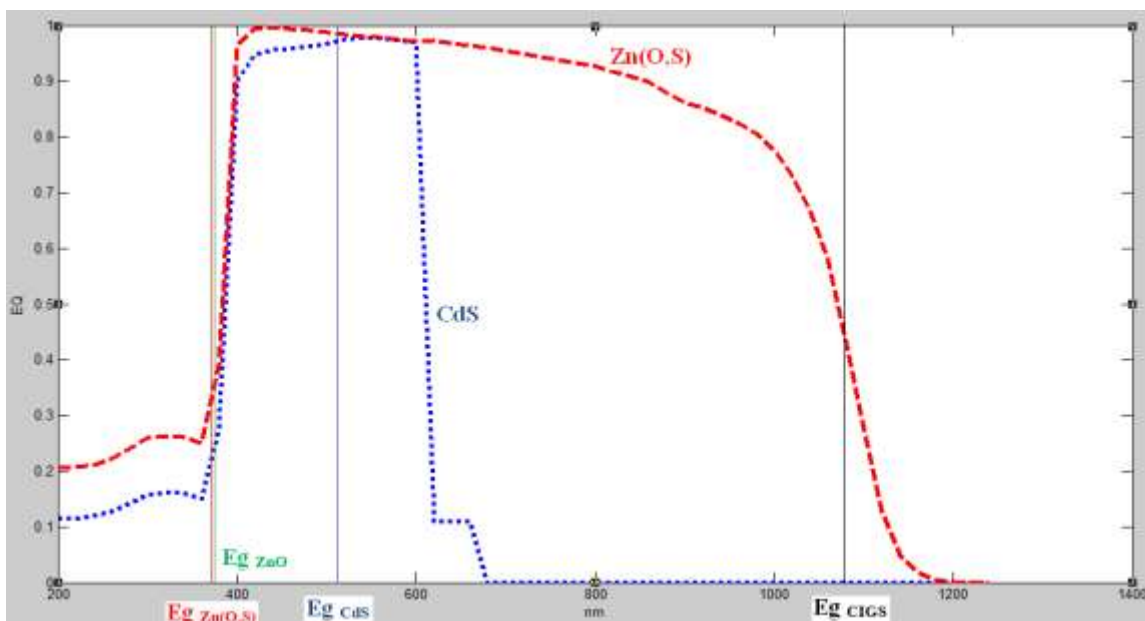


Fig. 2 :Quantum efficiency of the cell with CdS and Zn(O,S) buffer layers doped N with a donor doping density $N_d=10^{15} \text{cm}^{-3}$

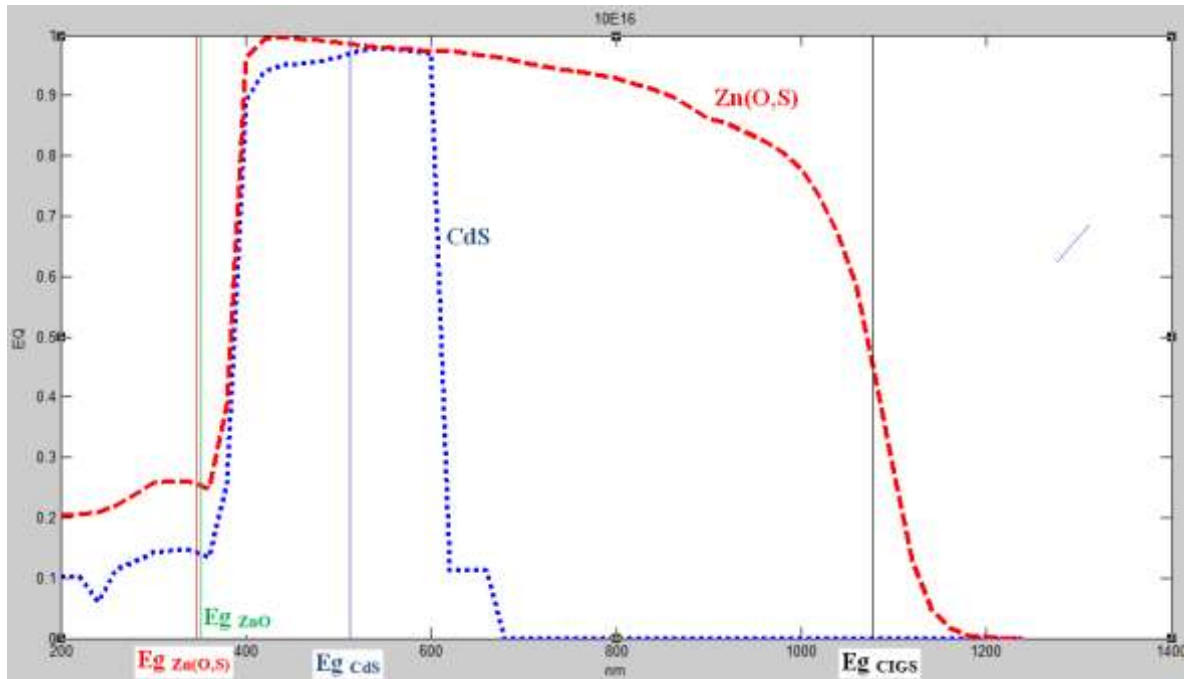


Fig. 3: Quantum efficiency of the cell with CdS and Zn(O,S) buffer layers doped N with a donor doping density $N_d=10^{16} \text{cm}^{-3}$.

The external quantum efficiency of the cell with a CdS buffer layer remains weak for wavelengths going from 200nm to 358nm. It let appear a minimum of 5.36% for $\lambda=238\text{nm}$. This minimum is due to a cliff noted on the CBO which represents a recombination center of photo generated carriers. From 358nm, the EQE increases quickly to reach a maximum of 98.21% for $\lambda=555\text{nm}$, which corresponds to an energy of 2.2eV. This maximum corresponds to the gap of CdS. The maximum absorption area extends until 600nm. This last is the wavelength from which external quantum efficiency falls and is reduced to zero with a wavelength of 680nm. This fall is due to a spike pronounced on the CBO which blocks clearly the photogenerated carriers.

As regards the quantum efficiency of the solar cell with a Zn(O,S) buffer layer we obtain a characteristic with a broader absorption area. For wavelengths going from 200nm to 358nm accompanied by significant energy, we have a weak EQE. When we pass the Zn(O,S) gap and the gap of the ZnO window layer, quantum efficiency increases quickly to reach a maximum of 100% with $\lambda=423\text{nm}$. This wavelength corresponds to an energy of 2,93eV. The maximum absorption area extends to the Cu(In, Ga)Se₂ gap. For the wavelengths higher than 1077nm, the creation of the carriers is minimal because the wavelengths are accompanied by energy lower than the gap of the Cu(In, Ga)Se₂ absorber layer. The quantum efficiency is reduced to zero for $\lambda=1188\text{nm}$. Then when we pass from the doping density of 10^{15}cm^{-3} to 10^{16}cm^{-3} , the EQE of the cell with a Zn(O,S) buffer layer remains more significant and less affected than that of the cell with CdS buffer layer.

C. External quantum efficiency of the cells with buffer layers doped $N_d=10^{17} \text{cm}^{-3}$.

The figure 4 gives the variation of quantum efficiency for the cells with CdS and Zn(O,S) buffer layers doped N with doping density of 10^{17}cm^{-3} . This doping density corresponds to strong doping level of the buffer layers.

We find with some differences the same characteristics as those obtained with the precedents doping densities of the buffer layers.

Compared to the quantum efficiency of the cell with a CdS buffer layer, for low incidental wavelengths, we don't observe decrease like previously with $N_d=10^{16} \text{cm}^{-3}$. However the EQE remains weak until $\lambda=355\text{nm}$, then it increases to reach a maximum by 98.7% for $\lambda=550\text{nm}$. This wavelength is accompanied by energy equal to 2.25eV. This energy is near to the CdS gap. The consequence of the spike noted on the CBO of the cell explains again the fall of quantum efficiency from $\lambda=600\text{nm}$. This fall continues until the cancellation of the EQE to an incidental wavelength of 680nm.

The quantum efficiency of the cell with a Zn(O, S) buffer layer presents a maximum absorption area broader than that obtained with CdS. There remains weak for wavelengths of 200nm with 355nm. Then it evolves to reach a maximum of 100% for a wavelength of 423nm which always corresponds to an energy of 2.93eV. As previously the EQE remains significant until near to the Cu(In, Ga)Se₂ gap. Then it drops to reduce to zero with $\lambda=1188\text{nm}$.

We observe that when we pass from a doping density of the buffer layers of 10^{16}cm^{-3} to 10^{17}cm^{-3} , the

quantum efficiency of the two types of cells is few affected.

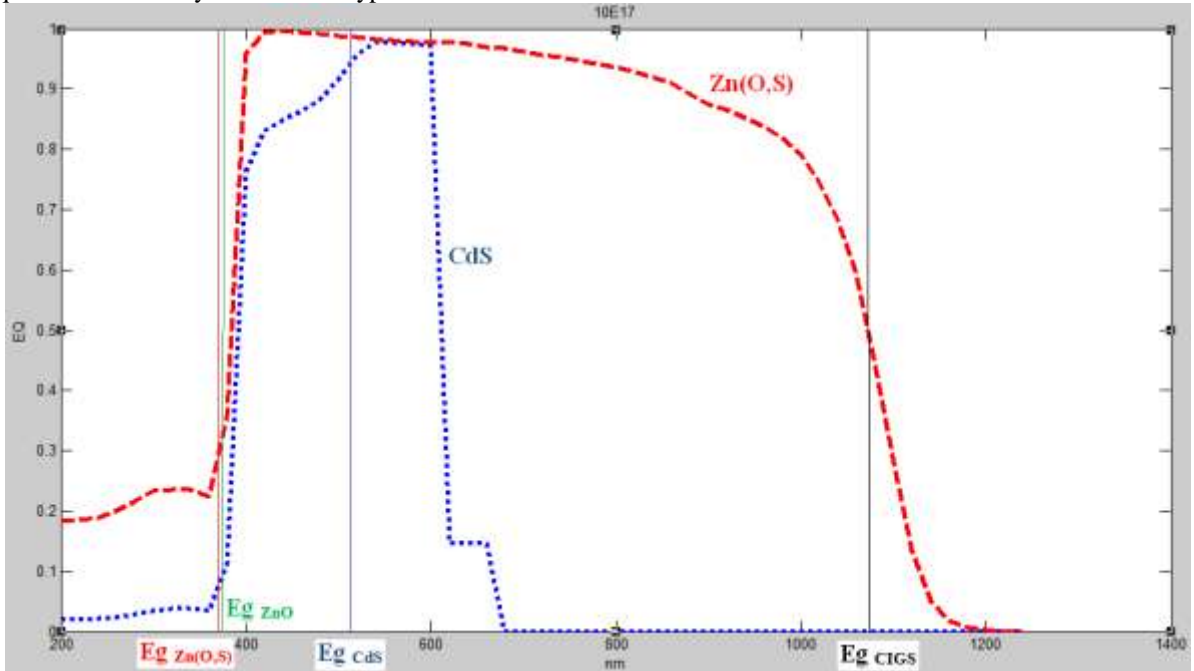


Fig. 4:Quantum efficiency of the cell with CdS and Zn(O,S) buffer layers doped N with a donor doping density $N_d=10^{17}cm^{-3}$.

D. External quantum efficiency of the cells with buffer layers doped $N_d=10^{18}cm^{-3}$.

The figure 5 gives the characteristics of the external quantum efficiency of the solar cells with CdS and Zn(O, S) buffer layers doped N with a doping density of $10^{18}cm^{-3}$. We are in a situation of strong levels of doping of the buffer layers. For the solar cell with a CdS buffer layer, we obtain a quantum efficiency which presents a very broad maximum absorption area. This area is about that of

the solar cell with Zn(O,S) buffer layer. For low wavelengths going from 200nm to 358nm, quantum efficiency remains weak. When we approach the gap of the ZnO window layer, it becomes significant and reaches a maximum of 98.5% for a wavelength of 541nm, which corresponds to an energy of 2.3eV. This energy is of the order of the gap of CdS. The spikes noted for the doping densities of $10^{15}cm^{-3}$ to $10^{17}cm^{-3}$ and which cause a fall of the EQE are not noted with a doping density of $10^{18}cm^{-3}$.

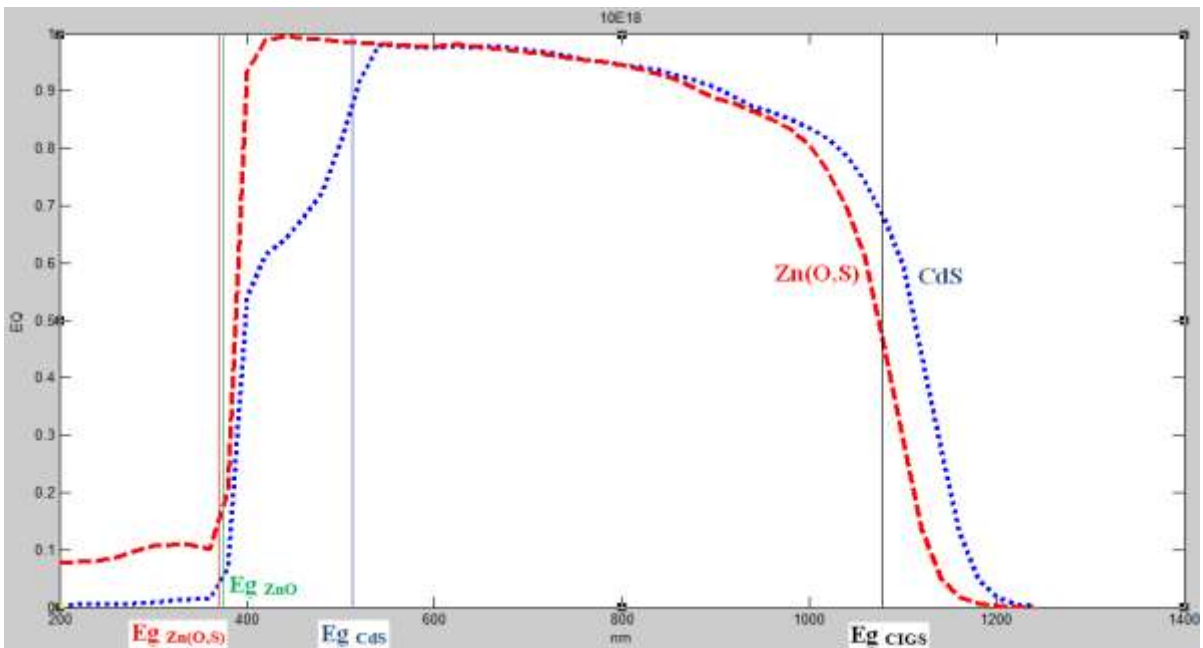


Fig. 5 :Quantum efficiency of the cell with CdS and Zn(O,S) buffer layers doped N with a donor doping density $N_d=10^{18}cm^{-3}$

Consequently the maximum absorption area increases clearly. Indeed the carriers photogenerated pass the CdS/Cu(In,Ga)Se₂ interface where they were blocked previously.

Concerning the quantum efficiency of the cell with a Zn(O,S) buffer layer, the characteristic is almost the same one. The doping density doesn't affect the quantum efficiency of this cell which reaches a maximum of 100%. This maximum is noted for an incidental wavelength equal to 440nm which corresponds to an energy of 2.8eV. For wavelengths going from 541nm to 828nm quantum efficiencies of the cells with CdS and Zn(O,S) buffer layers are quasi superposed. For wavelengths higher than 828nm, the EQE of the cell with CdS buffer layer is more significant than that of the cell with a Zn(O,S) buffer layer. This is due to the fact that the charge carriers photogenerated in the CuInGaSe₂ absorber layer cross more easily the CdS/Cu(In,Ga)Se₂ interface than the Zn(O,S)/Cu(In,Ga)Se₂ interface to be collected. The Quantum efficiencies drop gradually to reduce to zero with $\lambda=1200\text{nm}$ for Zn(O,S) and with $\lambda=1235\text{nm}$ for CdS. We note that when we pass from the medium doping levels at the high doping levels, the CdS becomes competing compared to Zn(O,S). With the donor doping density of 10^{18}cm^{-3} , the CdS presents a broader maximum absorption area in spite of the maximum quantum efficiency of 100% obtained with Zn(O,S).

E. External quantum efficiency of the cells with buffer layers doped $Nd=10^{19}\text{cm}^{-3}$.

The figure 6 gives the variations of the quantum efficiency of the cells with CdS and Zn(O,S) buffer layers doped N with a doping density of 10^{19}cm^{-3} . This doping density corresponds to a high level of doping.

We obtain characteristics different from those obtained with the precedents doping densities of

10^{18}cm^{-3} . The external quantum efficiencies of the cells remain weak from 200nm to 360nm. But for incidental wavelengths accompanied by energies higher than the gap of the ZnO window layer, the EQE increase quickly. They reach 99.3% with $\lambda=442\text{nm}$ for the cell with Zn(O, S) buffer layer and 98.6% with $\lambda=542\text{nm}$ for the cell CdS buffer layer. The quantum efficiency of the cell with the Zn(O,S) buffer layer is more significant than that of the cell with a CdS buffer layer until the wavelength of 542nm. For wavelengths higher than this value, the EQE are superposed and remained significant until to the Cu(In,Ga)Se₂ absorber layer. Then the quantum efficiencies drop and reduce to zero with $\lambda=1200\text{nm}$. From this wavelength, the incidental wavelengths are accompanied by too weak energy which can not generate carriers in Cu(In,Ga)Se₂ absorber layer which has a gap 2.4eV. We can say that for $Nd=10^{18}\text{cm}^{-3}$, the difference between the EQE characteristics is noted only for low incidental wavelengths lower than 542nm. For these low injection levels the quantum efficiency of the cell with Zn(O,S) buffer layer is more significant than that of the cell with a CdS buffer layer.

F. External quantum efficiency of the cells with buffer layers doped $Nd=10^{20}\text{cm}^{-3}$.

The figure 7 gives the variation of the external quantum efficiency of the solar cells with CdS and Zn(O,S) buffer layers doped N with a doping density of 10^{20}cm^{-3} . We are in a situation of surdopage of the buffer layers.

The characteristics obtained keep almost the same profiles but are shifted compared to the precedents doping densities. Compared to the cell with a CdS buffer layer, the EQE remains weak for low incidental wavelengths (200nm to 358nm).

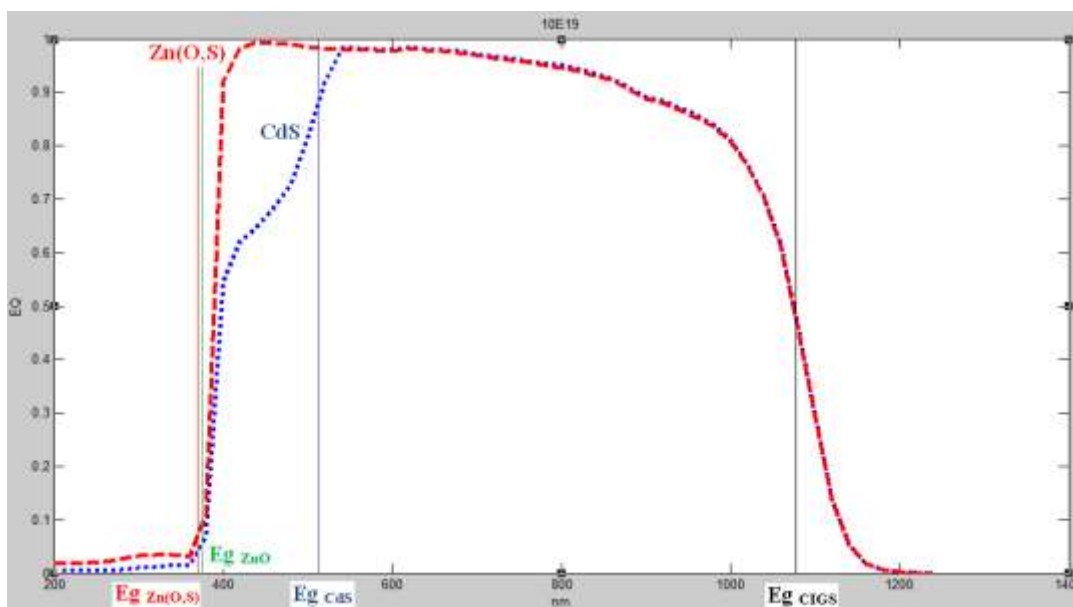


Fig. 6: Quantum efficiency of the cell with CdS and Zn(O,S) buffer layers doped N with a donor doping density $Nd=10^{19}\text{cm}^{-3}$.

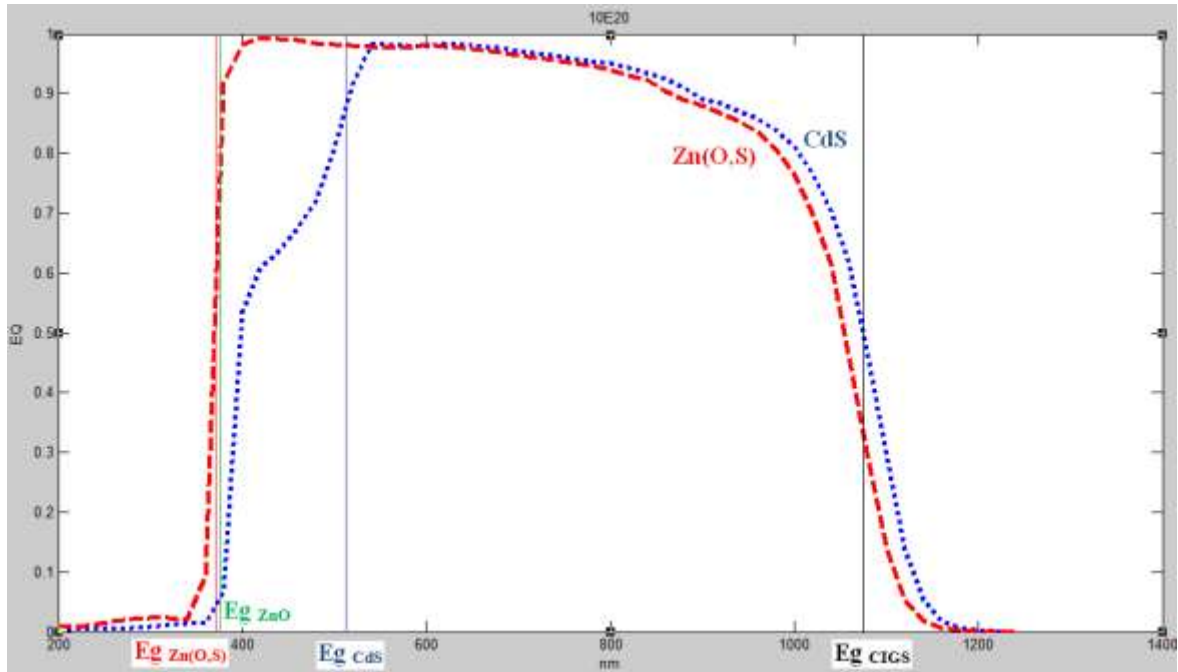


Fig. 7 :Quantum efficiency of the cell with CdS and Zn(O,S) buffer layers doped N with a donor doping density $N_d=10^{20}\text{cm}^{-3}$.

That of the cell with a Zn(O,S) buffer layer, which is also weak on this wavelengths range, starts increasing since we reach $\lambda=339\text{nm}$. It reaches a maximum of 99.2% for a wavelength of 423nm which is accompanied by an incidental energy of 2.9eV.

The EQE of the solar cell with a CdS buffer layer reaches a maximum of 98.2% for $\lambda=543\text{nm}$ which corresponds to an energy of 2.3eV. Since we pass the wavelength of 543nm, its quantum efficiency becomes more significant than that of the cell with a Zn(O,S) buffer layer. Then the variations of the two characteristics are almost identical. The quantum efficiencies drop to reduce to zero with a wavelength very close to 1200nm.

For $N_d=10^{20}\text{cm}^{-3}$ the two cells have the same amplitudes of the maximum absorption areas and present maxima close to 99.2% for Zn(O,S) and 98.2% for CdS.

IV. CONCLUSION

Former studies which were undertaken in our laboratory[13]-[14], gave results which are confirmed by the results published in this paper. The study of the quantum efficiency of the solar cells with CdS and Zn(O,S) buffer layers, shows us the interest of the use of Zn(O,S) in the place of CdS for the medium levels of donor doping densities up to 10^{17}cm^{-3} . We note a spike in the CBO of the cell with CdS buffer layer, which blocks the charge carriers photogenerated in the Cu(In,Ga)Se₂ thin film absorber layer. For the high doping levels, this effect is not noted and the two types of buffer layer give important properties of cell. At the end of this work we confirm that Zn(O,S) remains a preferential candidate for obtaining free-Cadmium solar cells.

REFERENCES

- [1] Zimmermann U., Ruth M., Edoff M., " Cadmium-free CIGS mini-modules with ALD-grown Zn(O,S)-based buffer layers. □ , Proc. Of the 21st European Photovoltaic Solar Energy Conference, Dresden 2006, 1831-1834.
- [2] D. Hariskos, R. Menner, P. Jackson, S. Paetel, W. Witte, W. Wischmann, M. Powalla, L. Bukert, T. Kolb, M. Oertel, B. Dimmler and B. Fuchs, " New reaction kinetics for a high rate chemical bath deposition of the Zn(O,S) buffer layer for Cu(In,Ga)Se₂ based solar cells. □ , Prog. Photovolt.: Res. Appl., Early Review, 31 Jan. 2012.
- [3] Okamoto A., Minemoto T., Takakura H., " Application of sputtered ZnO_{1-x}S_x buffer layers for CuInGaSe₂ solar cells. □ , Japanese Journal of Applied Physics 2011; 50:04DP10-1-04DP10-4, DOI: 10.1143/JJAP.50.04DP10.
- [4] Samaneh Sharbati and James R. Sites, " Impact of the Band Offset for n-Zn(O,S)/p-Cu(In,Ga)Se₂ solar cells. □ , IEEE Journal of Photovoltaics, Vol. 4, No 2, March 2014.
- [5] C. Platzer-Bjorkmann, T. Torndahl, D. Abou-Ras, J. Molsmstrom, J. Kessler and L. Stolt, " Cu(In,Ga)Se₂/Zn(O,S) solar cells: band alignment and sulfure gradient. □ , J. Appl. Phys., Vol. 100, pp 044506-1-044506-9, 2006.
- [6] K. Ramanathan, J. Mann, S. Glymm, S. Christensen, J. Pankow, J. Li, J. Scharf, L. Mansfield, M. Contreras and R. Noufi, " Comparative study of the Zn(O,S) buffer layers and CIGS solar cells fabricated by CBD, ALD and sputtering. □ , in Proc. 38th IEEE Photovoltaic Spec. Conf., Austin, T. X., USA, June 2012.
- [7] M. Powella, Zentrum fur Sonnenenergie-und Wassertoff-Forschung Baden-Wuerttemberg, Germany, WWW.pv-tech.org, August 29th 2010.
- [8] Tao Song, " Distorsion to current-voltage curves of CIGS cells with sputtered Zn(O,S) buffer layers. □ , Colorado State University, 2013.
- [9] Marie Buffiere, " Synthèse et caractérisation des couches minces de Zn(O,S) pour application au sein des cellules solaires à base de Cu(In,Ga)Se₂. □ , Materials, Université de Nantes, 2011.
- [10] A. K. Ehemba, M. Dieng, D. Diallo, D. Wade and M. Soce, " The influence of the type and the thickness of the window layer on the electric parameters of the Cu(In,Ga)Se₂ thin film solar cell. □ , The International Journal of Engineering and Science (IJES), Vol. 4, Issue 10, pp 81-86, 2015.
- [11] Yiming Liu, Daniel Henzel an Angus Rockett, " A revised version of the AMPS simulation code. □ , Bourses d'Etat

- Université de Nankai, à Tianjin, Chine et Université de l'Illinois, Urbana, Etats-Unis.
- [12] Nina E. Gorji, Ugo Reggiani and Leonardo Sandrolini, " A simple model for the photocurrent density of a graded band gap CIGS thin film solar cell.", *Solar Energy* 86(2012), pp 920-925.
- [13] O. A. Niasse, B. Bengue, B. Ba, A. Ndiaye and I. Youm, " Effets des excitons sur le rendement quantique de la cellule solaire CdS/CdTe par le model de la fonction dielectrique.", *Revue des Energies Renouvelables*, Vol. 12, N°3, (2009), pp 501-512.
- [14] Moulaye Diagne, Nacire Mbengue, Mamadou Niane, Omar .A. Niasse, Bassirou Ba "External Quantum Efficiency of a Solar Cell ZnO/CdTe: Effect of Emitter and Base Thicknesses.", *International Journal of Engineering Trends and Technology (IJETT) – Volume 20 Number 2 – Feb 2015*.